

# Liquid Crystalline Carborane Diester Molecules: Structure and Ultraviolet Absorption Behavior based on DFT and Semiempirical Methods

T. Jaison Jose<sup>1</sup>, A. Simi<sup>2</sup>, M. David Raju<sup>3</sup>, P. Lakshmi Praveen<sup>4</sup>

P. G. Department of Chemistry, Andhra Loyola College, Vijayawada, Andhra Pradesh, India. <sup>1</sup>

Department of Chemistry, St. Joseph's College, Tiruchirapalli, Tamil Nadu, India. <sup>2</sup>

P. G. Department of Chemistry, P. B. Siddhartha College of Arts & Sciences, Vijayawada, Andhra Pradesh, India. <sup>3</sup>

Department of Physics, Veer Surendra Sai University of Technology, Burla, Odisha, India. <sup>4</sup>

**Abstract:** The absorption behaviour of carborane diester liquid crystals viz., bis(4-propyloxyphenyl) 1,12-dicarba-closo-dodecaborane-1,12-dicarboxylate ( $C_{22}H_{32}B_{10}O_6$ ), and bis(4-butoxyphenyl) 1,10-dicarba-closo-decaborane-1,10-dicarboxylate ( $C_{24}H_{34}B_8O_6$ ) have been studied in ultraviolet (UV), and visible (Vis) regions. Structure of these nematogenic molecules have been optimized using the Density functional B3LYP with 6-31+G (d) basis set using crystallographic geometry as input. Molecular charge distribution and phase stability of these systems have been analyzed based on Mulliken and Loewdin population analysis. The electronic absorption spectra of the molecules have been simulated by employing the DFT method, semiempirical CNDO/S and INDO/S parameterizations. The UV absorption behaviour and stability of the molecules has been discussed based on the absorption spectra data, and group charge distributions.

**Key words:** Liquid crystal; UV-Visible spectra; Oscillator strength; Phase stability.

## I. INTRODUCTION

Liquid crystal displays (LCDs) lead the market for flat panel displays, especially for handy applications. The focus towards the molecular structure can provide information on stability of the mesophase that influence greatly the physical properties. The need to develop new liquid crystalline (LC) compounds, for desired applications and technology provides a new motivation to develop a deeper understanding in structure-stability relationship [1]. Even though advances in synthesis and characterization explore many achievements, it is often desirable; to establish a logic of phase stability-material behaviour prior to synthesis [2].

In designing new LC molecules, besides carbon, boron is the only other element that can build molecules of unlimited size by covalently bonding to itself. Boron has only three valence electrons, prefers to adopt cluster motifs. The *closo* prefix in the title compounds defines a cluster that either has triangular faces or no missing vertices. *closo*-Boranes are characterized by high thermal and oxidative stability due in part to highly delocalized bonding within a  $\sigma$ -framework [3]. This type of bonding is not much different than that of the three-dimensional aromatic benzene  $\pi$ -framework. Since boron is electron deficient, it forms three centre two-electron bonds, and this is the foundation for the  $\sigma$ -framework. The 3D cage geometry and special electronic properties of boron clusters make them potentially attractive structural elements of novel LC materials [4]. Their thermal stability, delocalized bonding, and ease of functionalisation have the potential to alter the electronic

structure, and therefore response of the bulk LC material to external stimuli.

Ultraviolet (UV) absorption behavior of LCs is significant, as they maintain the ability to interact with light. Such properties are desirable in the design of new LC materials to achieve high electronic polarizability, low anisotropy, which would result in low birefringence [5], and a high isotropic refractive index [6] for a boron containing LC [7]. These clusters also have large molecular size, high symmetry axes, when compared to benzene and bicyclo[2.2.2]octane [8]. The calculation of UV-Vis spectra is appealing since a large number of methods have been employed to calculate the absorption wavelength and oscillator strength of electronic transitions.

The methods based on Time Dependent Density Functional Theory (TDDFT) applied to small and middle sized systems provide rather good accuracy at low computational cost [9]. These methods still remain of rather limited application for establishing realistic molecular models and biological systems. Hence, the alternate use of semiempirical schemes has an extensive use to analyze absorption behaviour. Such approaches allow for the calculation of electronic transitions between the ground state and the different excited states, which gives the energies of the corresponding radiations.

Subtle changes in the molecular structure of molecules lead to great variations of both physical properties like stability, optical and electronic properties such as absorption behaviour, energy gap, electron affinity etc.

In view of this, the present manuscript aims at providing a comparative picture of structural and optical properties of nematogenic  $C_{22}H_{32}B_{10}O_6$ , and  $C_{24}H_{34}B_8O_6$  using semiempirical CNDO/S (complete neglect of differential overlap/ spectroscopy) [10-14], INDO/S (intermediate neglect of differential overlap/ spectroscopy) [15, 16] schemes and DFT method. The HOMO (Highest Occupied Molecular Orbital)/ LUMO (Lowest Unoccupied Molecular Orbital) energies, oscillator strength ( $f$ ) have also been reported using these three methods. An examination of crystal structure data has revealed that  $C_{22}H_{32}B_{10}O_6$ , and  $C_{24}H_{34}B_8O_6$  molecules exhibit nematic-isotropic (N-I) transition temperatures at 468K, and 456.4K respectively [8].

## II. CALCULATION METHODS

In the present analysis, three methods have been employed to calculate the UV absorption spectra of carborane diester molecules  $C_{22}H_{32}B_{10}O_6$ , and  $C_{24}H_{34}B_8O_6$ .

### 2.1 DFT Method

The first method is based on DFT theory. An understanding of absorption behaviour requires the knowledge of molecular orbitals properties, spectral shifts, and appropriate excited states. Moreover, their photophysics, and chemistry represent a challenge in understanding of the excited states dynamics. The main difficulties against reliable theoretical models are concerned with the size of systems, and the presence of strong electron correlation effects. Both properties are difficult to treat in the framework of the quantum mechanical methods rooted in the Hartree-Fock (HF) theory. Density functional theory (DFT) is successful to evaluate a variety of ground-state properties with accuracy close to that of post-HF methods [17, 18].

An important factor that determines the accuracy of TDDFT excitation energies is the exchange correlation functional used in the calculation. The use of these hybrid functionals yields good accounts of the vertical excitation energies of the excited states with substantial charge transfer character. In this context, The B3LYP (Becke-Lee-Yang-Parr) version of DFT is the combination of Becke's three parameter non-local hybrid functional of exchange terms [19] with the Lee, Yang and Parr correlation functional [20]. The basis set of 6-31+G (d) contains a reasonable number of basis set functions that are able to reproduce the experimental data. As a consequence, there is currently a great interest in extending DFT to excited electronic states. The TDDFT approach offers a rigorous route to the calculation of vertical electronic excitation energies, and other spectral characteristics [9].

### 2.2 CNDO/S – CI and INDO/S – CI Methods

The other two methods are based on semiempirical approximations CNDO/S, and INDO/S. The ground state of a closed-shell system is generally well represented by a single determinantal wave function. However, for an accurate representation of excited states full CI calculations are required. The corresponding calculations

of molecules have been made using the CNDO/S, and INDO/S methods. In these two methods, the wave functions of the ground, and once electronically excited states of  $\pi\pi^*$ -type for a molecule have been calculated in the one-configurational approximation. The electronic absorption spectrum has been calculated using the method of CI on the basis of obtained multi-electron wave functions of molecules. In the CIS approach, orbitals of the H-F solution have been used to generate all singly excited determinants of the CI expansion. This treatment can be thought as the H-F method for excited states.

It is important to note here that semiempirical MO method has always been calibrated using a set of trial functions. In addition to the shortcomings, which result from the inherent structure of the method due to the particular approximations, use of the different set of trial functions may require a reparameterization of the method. The ZINDO [16, 21, 22] has been specifically parameterized to give the theoretical transition energies and the respective intensities of molecules in the UV range with a given CI expansion of singly excited determinants. The electronic configurations considered here are generated by promoting one electron from the HOMO to the LUMO. Further, the introduction of levels has been performed to test the validity of our approach, and it does not change the results significantly. The scaling of the CI space [23] should correct somewhat for the size extensivity error of the CI. Furthermore, the results obtained by using a larger CI for smaller systems show little dependence on the CI space.

### 2.3 Molecular Structures

The present theoretical models comprise of the carborane diester molecules viz.,  $C_{22}H_{32}B_{10}O_6$ , and  $C_{24}H_{34}B_8O_6$ . The geometries optimizations have been performed using the DFT approach, the hybrid functional B3LYP [20], exchange-correlation functional, and the 6-31+G (d) basis set. The DFT approach was originally developed by Hohenberg and Kohn [21], Kohn and Sham [24, 25] to provide an efficient method of handling the many-electron system. The theory allows us to reduce the problem of an interacting many-electron system to an effective single-electron problem. On the basis of the DFT geometries, the electronic structures, excitation energies, and excited state wave functions have been calculated coupled with the configuration interaction (CI) single level of approximation including all  $\pi\rightarrow\pi^*$  single excitations. This has been found adequate to determine the UV-Visible absorption spectra provided that the suitable parameterizations are used. For the calculation of absorption spectra, the CI method is widely employed. Using a CI method in combination with a semi-empirical model Hamiltonian, an evaluation of absorption spectra of large organic molecules, and LCs becomes possible. Hence, we employed the CNDO/S – CI and INDO/S – CI methods including all valence electrons, and applied for the calculation of electronic spectra of the molecules. In the present work, a comparative analysis has been carried out by employing the CNDO/S, INDO/S, and DFT methods to calculate the UV-Vis absorption spectrum. The DFT calculations have been performed by a spectroscopy

oriented configuration interaction procedure (SORCI) [26], however, a revised version of QCPE 174 by Jeff Reimers, University of Sydney, and coworkers have been used for the semiempirical calculations. The general structural parameters of the systems such as bond lengths and bond angles have been taken from the published crystallographic data [8] to construct the electronic structures. Calculation of absorption spectra for the title molecules have been carried out.

### III. RESULTS AND DISCUSSION

The molecular structures of  $C_{22}H_{32}B_{10}O_6$  and  $C_{24}H_{34}B_8O_6$  molecules have been shown in Fig. 1. The molecular charge distribution, and phase stability of the molecules has been correlated as given below:

#### 3.1 Molecular Charge Distribution

In general, the increase in molecular flexibility leads to a decrease of phase stability presumably due to the lower packing density in the LC phase. It is expected that the specific charge distributions in LC molecules play an influential role in the formation of various mesophases. An appropriate modeling of this fundamental molecular feature relies on the possibility of assigning a partial charge to all atomic centers. To parameterize the molecular level computational studies, partial charges are helpful. Quantum chemical computations offer the possibility to take a detailed look at the electronic structure of the molecules. This can be done, by determining atom-based partial charges.

Since group charges are needed to explain the behaviour of mesogens, Mulliken population analysis, which partitions the total charge among the atoms in the molecule, has been performed, and the results have been compared with those obtained from Loewdin population analysis. Much agreement between the methods has been found in terms of the group charges of each molecule. It is evident from Table 1 that the positively charged alkyl chains of  $C_{22}H_{32}B_{10}O_6$  will be strongly attracted by the negatively charged side group as well as the core, causing the formation of longer units in the nematic phase. Hence, the nematic phase stability is expected to be high for  $C_{22}H_{32}B_{10}O_6$ . Further, the thermal vibration amplitude of the chain carbon atoms increase markedly with the increase of chain length, indicating a low packing efficiency for  $C_{24}H_{34}B_8O_6$ . This leads to the drastic decrease in nematic phase stability. This is in agreement with the N-I transition temperatures reported by the crystallographer (Table 1).

#### 3.2 UV-Visible Absorption Spectrum

Increasing the number of carbon atoms in the end chain is the widely used technique to alter the physical properties of LC molecules. The description of molecular quantities by quantum chemical methods underlies some principle restrictions [27], *i.e.* there exists a compromise between the complexity of the systems studied and the accessible theoretical accuracy. For the calculation of electronic spectra, the configuration interaction (CI) method is widely employed. Using a CI method in combination with

a semi-empirical model Hamiltonian, an evaluation of absorption spectra of large organic molecules and LCs becomes possible. The principal absorption bands in the molecules are due to the  $\pi \rightarrow \pi^*$  transitions in the core part (the cage like structure in this case) of the molecule. In general, transitions are roughly conserved in the model systems studied, but they are influenced by the conjugation length, degree of conjugation, and the different substituents.

The present calculations have been carried out on carborane diester molecules viz.,  $C_{22}H_{32}B_{10}O_6$ , and  $C_{24}H_{34}B_8O_6$  to study their UV stability in the light of the shift of absorption wavelength, and the corresponding spectral data. The variation in the absorption spectra has been observed due to the increment of carbon atoms in the end and side groups. The detailed picture of absorption spectra of isolated molecules based on TDDFT calculations have been given below. Further, the spectral data based on all the three schemes have been reported in Table 2 and Table 3.

#### $C_{22}H_{32}B_{10}O_6$ :

The absorption spectrum of  $C_{22}H_{32}B_{10}O_6$  is shown in Fig. 2 based on the three methods. The DFT data shows that three strong absorptions at 204.69nm ( $\lambda_1$ ), 239.84nm ( $\lambda_2$ ), and 271.48nm ( $\lambda_3$ ) have been observed in the UV region. However, no absorption has been observed in the visible region. The strongest band appears in a region of 200nm to 216.99nm with absorption maxima ( $\lambda_{max}$ ) at 204.69nm ( $\lambda_3$ ). This band arises from the HOMO  $\rightarrow$  LUMO transition and is assigned as  $\pi \rightarrow \pi^*$  transitions in the molecule. The oscillator strength ( $f$ ) values corresponding to three wavelengths are 0.11, 0.09, and 0.03 respectively. Further, the calculation also predicts  $\pi \rightarrow \pi^*$  transitions corresponding to weak absorption bands at remaining two wavelengths ( $\lambda_2$  and  $\lambda_3$ ).

#### $C_{24}H_{34}B_8O_6$ :

Fig. 3 shows the absorption spectra of  $C_{24}H_{34}B_8O_6$  using the three methods. The DFT data shows three prominent bands in the UV region with strong absorptions at 205.27nm ( $\lambda_1$ ), 242.77nm ( $\lambda_2$ ), and 273.24nm ( $\lambda_3$ ). The strongest band has been observed from 200nm to 217.58nm with absorption maxima at 205.27nm. However, no absorption has been observed in the visible region. This band arises due to the HOMO  $\rightarrow$  LUMO transition and is assigned as  $\pi \rightarrow \pi^*$  transitions in the molecule. The oscillator strength ( $f$ ) values corresponding to three wavelengths are 0.14, 0.10, and 0.03 respectively. However, the other weak absorption bands at  $\lambda_2$  and  $\lambda_3$  also indicate the possibility of additional  $\pi \rightarrow \pi^*$  transitions.

Thus, for  $C_{22}H_{32}B_{10}O_8$  substitution of additional alkyl group on both sides (forming  $C_{24}H_{34}B_8O_6$ ) leads to a bathochromic shift (the shift of absorption maxima to a longer wavelength). Further, increment in the alkyl chain length shows hyperchromic effect (increment in absorbance). The shift may be understood due to the ease of transfer of electrons through the conjugated system with increase in size and planarity of the molecules. Further,

due to this, a decrement has been found in optical gap. Evidently, both the DFT and INDO/S methods show a good agreement in exhibiting the shift of absorption wavelength. The tendency of absorption wavelength with respect to the substitution of additional alkyl group is the same in both methods. However, a deviation in shift of absorption maxima has been observed for both molecules using the CNDO/S method. A comparative picture of the vertical excited energy ( $E_V$ ), and the oscillator strength ( $f$ ) corresponding to absorption maxima ( $\lambda_{max}$ ) using the CNDO/S, INDO/S, and TDDFT methods have been reported in Table 2. The lower chain length causes higher transition energy. In view of this, it may be understood that calculated vertical excitation energies are relatively sensitive to the method, and the end chain length. Evidently, the electronic transitions among the methods reveal that the maximum oscillator strength is exhibited by  $C_{24}H_{34}B_8O_6$  molecule in UV range at longer wavelength side (Table 2). Further, the absorption maxima of  $C_{24}H_{34}B_8O_6$  is higher as per the DFT and CNDO/S data. However, a little deviation has been observed in case of INDO/S data. Hence, the UV stability and the flexibility for electronic transitions of  $C_{24}H_{34}B_8O_6$  are higher, which may be exploited for several optoelectronic applications.

The oscillator strength is a dimensionless quantity that expresses the probability of absorption of electromagnetic radiation in transitions between energy levels of an atom or molecule. It indicates the allowedness of electronic transitions in a molecule, and it is particularly valuable as a method of comparing 'transition strengths' between different types of quantum mechanical systems. A graph has been plotted between wavelength, and oscillator strength (Fig. 4) to understand the intensity profiles of the compounds. It may be observed from the figure that  $C_{22}H_{32}B_{10}O_6$  exhibits the highest oscillator strength at 202.70nm, while  $C_{24}H_{34}B_8O_6$  at 203.90nm. Further, these molecules exhibit the last intensity peak around 277.50nm, and 284.30nm respectively. This indicates the much flexibility of  $C_{24}H_{34}B_8O_6$  for electronic transitions over a long wavelength region, which causes high photo sensitivity. The continuous decrease in absorption (Fig. 2, 3), and oscillator strength (Fig. 4) clearly indicates the breakage of aromatic rings with respect to the higher wavelengths, and subsequently losing the photo sensitivity. This decrease in absorption as a function of increasing UV-Visible wavelength has been consistently observed for both the molecules.

#### IV. HOMO-LUMO ANALYSIS

The HOMO level can be thought the outermost orbital containing electrons, tends to give these electrons such as an electron donor. On the other hand; LUMO can be thought the innermost orbital containing free places to accept electrons [28]. Owing to the interaction between HOMO and LUMO orbital of a structure, transition of state  $\pi \rightarrow \pi^*$  type is observed with regard to the molecular orbital theory. Therefore, while the energy of the HOMO is directly related to the ionization energy, LUMO energy is directly related to the electron affinity. Energy difference between HOMO and LUMO orbital is called as

energy gap, which is an important factor for analyzing the stability of the structures. The chemical hardness is, a measure for resistance to deformation or change, is very important tool to study the stability of molecular systems, and is also an approximation to the first electron excitation energy. The lowering of energy separation between the HOMO and LUMO clearly explicates the charge transfer interactions taking place within the molecule. The average value of the HOMO and LUMO energies is related to the electro negativity. The negative of the electro negativity is the chemical potential ( $\mu$ ).

A comparison of HOMO, LUMO energies, energy gap ( $E_g$ ) values, Ionization energy, Electron affinity, Chemical hardness, Electronic chemical potential, Electrophilicity index, and softness of isolated molecules have been made as reported in Table 3. Evidently, the molecules exhibit much agreement between DFT and INDO/S methods. The HOMO value of  $C_{24}H_{34}B_8O_6$  is higher, due to the longer shift  $\lambda_{max}$  after substitution. However, the energy gap ( $E_g$ ) shows a preference with increment in end alkyl groups. The increment of alkyl groups in the end chain causes a decrement in optical gap  $E_g$ , thereby increasing the conductivity of the molecule. Further, the soft molecule ( $C_{24}H_{34}B_8O_6$ ) has a small energy band gap, but hard molecule ( $C_{22}H_{32}B_{10}O_6$ ) has a large one. Hence, these parameters also confirm the high flexibility of  $C_{24}H_{34}B_8O_6$ . Further, since, the energy gap determines the molecular reactivity such as the ability to absorb light, and to react with other species, a molecule with small gap ( $C_{24}H_{34}B_8O_6$  in this case) is expected to have higher reactivity, and a lower stability in photo-physical processes.

#### V. CONCLUSION

The present comparative analysis on carborane diester molecules based on DFT and semiempirical methods leads to the following conclusions:

1. The phase stability is expected to be high for  $C_{22}H_{32}B_{10}O_6$  from charge distribution analysis, which is in agreement with crystallographic result.
2. The increase in molecular flexibility leads to a decrease of phase stability presumably due to the lower packing density in the LC phase for  $C_{24}H_{34}B_8O_6$ .
3. The red shift may be understood due to the ease of transfer of electrons through the conjugated system with increase in size and planarity of the  $C_{24}H_{34}B_8O_6$  molecule. Further, due to this, a decrement has been found in optical gap.
4. The intensity profile studies confirm high UV stability, and flexibility of  $C_{24}H_{34}B_8O_6$ . Further, the softness parameters, and the energy gap values are in agreement with this observations.

#### REFERENCES

- [1] Lakshmi Praveen, P.; Ojha, D.P. Estimation of configurational entropy and stability of nematic phase in mesogens-Role of molecular interactions. *J. Mol. Liq.* 2011, 158, 27-32.
- [2] Lakshmi Praveen, P.; Ojha, D. P. Calculation of spectral shifts in UV-visible region and photoresponsive behaviour of fluorinated liquid crystals: Effect of solvent and substituent. *Mat. Chem. Phys.* 2012, 135, 628-634.

- [3] Grimes, R. N. Boron clusters come of age. *J. Chem. Ed.* 2004, 81, 658–672.
- [4] Jankowiak, A.; Balinski, A.; Harvey, J. E.; Mason, K.; Januszko, A.; Kaszynski, P.; Young Jr. c, V. G.; Persoons, A. [closo-B<sub>10</sub>H<sub>10</sub>]2- as a structural element for quadrupolar liquid crystals: a new class of liquid crystalline NLO chromophores. *J. Mat. Chem. C.* 2013, 1, 1144-1159.
- [5] Kaczmarczyk, A.; Kolski, G. B. Polarizability of the closed-cage boron hydride B<sub>10</sub>H<sub>10</sub><sup>2-</sup>. *J. Phys. Chem.* 1964, 68, 1227–1229.
- [6] Kaczmarczyk, A.; Kolski, G. B. The polarizabilities and diamagnetic susceptibilities of polyhedral boranes and haloboranes. *Inorg. Chem.* 1965, 4, 665–671.
- [7] Ringstrand, B. Boron clusters as structural elements of novel liquid crystalline materials. *Liq. Cryst. Today.* 2013, 22, 22-35.
- [8] Kaszynska, P.; Januszko, A.; Ohtab, K.; Nagamine, T.; Potaczeka, P.; Young Jr. C, V. G.; Endo, Y. Conformational effects on mesophase stability: numerical comparison of carborane diester homologous series with their bicyclo[2.2.2]octane, cyclohexane and benzene analogues. *Liq. Cryst.* 2008, 35, 1169-1190.
- [9] Nataraj, A., Balachandran, V.; Karthick, T. Molecular structure, vibrational spectra, first hyperpolarizability and HOMO–LUMO analysis of p-acetylbenzoinitrile using quantum chemical calculation. *J. Mol. Struct.* 2013, 1038, 134-144.
- [10] Bene, J. D.; Jaffe, H. H. Use of the CNDO method in spectroscopy. I. benzene, pyridine, and the diazines. *J. Chem. Phys.* 1968, 48, 1807-1813.
- [11] Bene, J. D.; Jaffe, H. H. Use of the CNDO method in spectroscopy. II five-membered rings. *J. Chem. Phys.* 1968, 48, 4050-4055.
- [12] Bene, J. D.; Jaffe, H. H. Use of the CNDO method in spectroscopy. III. Mono substituted benzenes and pyridines. *J. Chem. Phys.* 1968, 49, 1221-1229.
- [13] Bene, J. D.; Jaffe, H. H. Use of the CNDO method in spectroscopy. IV. small molecules: spectra and ground state properties. *J. Chem. Phys.* 1968, 50, 1126-1129.
- [14] Ellis, R. L.; Kuehnlenz, G.; Jaffe, H. H. The use of CNDO method in spectroscopy. *Theor. Chim. Acta.* 1972, 26, 131-140.
- [15] Bacon, A. D.; Zerner, M. C. An intermediate neglect of differential overlap theory for transition metal complexes: Fe, Co and Cu chlorides. *Theor Chim Acta.* 1979, 53, 21-54.
- [16] Zerner, M. C.; Loew, G. H.; Kirchner, R. F.; Westerhoff, U. T. M. An intermediate neglect of differential overlap technique of transition-metal complexes. *J. Am. Chem. Soc.* 1980, 102, 589-599.
- [17] Stratmann, R. E.; Scuseria, G. E.; Frisch, M. J. An efficient implementation of time- dependent density functional theory for the calculation of excitation energies of large molecules. *J. Chem. Phys.* 1998, 109, 8218-8224.
- [18] Neugebauer, A., Hafelinge, G. Reliability of *ab-initio* methods and basis set dependencies for accurate prediction of r<sub>e</sub> distances of CO bond lengths, *J. Mol. Struct. Theochem.* 2002, 585, 35-47.
- [19] Cornaton, Y.; Franck, O.; Teale, A. M.; Fromager, E. Analysis of double hybrid density functionals along the adiabatic connection. *Mol. Phys.* 2013, 111, 1275-1294.
- [20] Lee, C.; Yang, W.; Parr, R. G. Development of the Colle-Salvetti correlation-energy formula into a functional of the electron density. *Phys. Rev. B.* 1988, 37, 785-789.
- [21] Hohenberg, P.; Kohn, W. Inhomogeneous electron gas. *Phys. Rev.* 1965, 136, B864-B871.
- [22] Head, J. D., Zerner, M. C. An approximate hessian for geometry optimization, *Chem. Phys. Lett.* 1986, 131, 359-366.
- [23] Edwalds, W. D., Zerner, M. C. A generalized restricted fock-operator, *Theor. Chim. Acta.* 1987, 72, 347-361.
- [24] Kohn, W., Sham, L. J. Self-consistent equations including exchange and correlation effects, *Phys. Rev.* 1965, 140, A1133-A1188.
- [25] Jones, R. O.; Gunnarsson, O. The density functional formalism, its application and prospects. *Rev. Mod. Phys.* 1989, 61, 689-746.
- [26] Neese, F. A. A spectroscopy oriented configuration interaction procedure. *J. Chem. Phys.* 2003, 119, 9428-9444.
- [27] Targema, M., Egbdi, M. O. O., Adeyoe, M. D. Molecular structure and solvent Effects on the dipole moments and polarizabilities of some aniline derivatives, *Comp. Theor. Chem.* 2013, 1012, 47-53.
- [28] Gayathri, H. N., Suresh, K. A. Electrical conductivity in Langmuir-blodgett films of n-alkyl cyanobiphenyls using current sensing atomic microscope, *J. Appl. Phys.* 2015, 117, 245311: 1-7.

### FIGURES CAPTION

Fig. 1: The molecular structures of (a) C<sub>22</sub>H<sub>32</sub>B<sub>10</sub>O<sub>6</sub>, and (b) C<sub>24</sub>H<sub>34</sub>B<sub>8</sub>O<sub>6</sub> molecules.

Fig. 2: Absorption spectra of C<sub>22</sub>H<sub>32</sub>B<sub>10</sub>O<sub>6</sub> molecule using DFT, CNDO/S, and INDO/S approximations. Extinction unit: 10<sup>4</sup> dm<sup>3</sup> mol<sup>-1</sup> cm<sup>-1</sup>

Fig. 3: Absorption spectra of C<sub>24</sub>H<sub>34</sub>B<sub>8</sub>O<sub>6</sub> molecule using DFT, CNDO/S, and INDO/S approximations. Extinction unit: 10<sup>4</sup> dm<sup>3</sup> mol<sup>-1</sup> cm<sup>-1</sup>

Fig. 4: Intensity profiles of C<sub>22</sub>H<sub>32</sub>B<sub>10</sub>O<sub>6</sub>, and C<sub>24</sub>H<sub>34</sub>B<sub>8</sub>O<sub>6</sub> molecules using DFT method.

Table 1. Mulliken (M) and Loewdin (L) group charges and nematic-isotropic transition temperatures for C<sub>22</sub>H<sub>32</sub>B<sub>10</sub>O<sub>6</sub>, and C<sub>24</sub>H<sub>34</sub>B<sub>8</sub>O<sub>6</sub> molecules.

Molecule	Side Group		Core		Alkyl		T <sub>N-I</sub> /K [8]
	M	L	M	L	M	L	
C <sub>22</sub> H <sub>32</sub> B <sub>10</sub> O <sub>6</sub>	-0.39	-0.34	-0.25	-0.18	0.63	0.52	468
C <sub>24</sub> H <sub>34</sub> B <sub>8</sub> O <sub>6</sub>	-0.40	-0.35	-0.21	-0.17	0.61	0.52	456.4

Table 2. The vertical excited energy (E<sub>v</sub>), and oscillator strength (f) of C<sub>22</sub>H<sub>32</sub>B<sub>10</sub>O<sub>6</sub>, and C<sub>24</sub>H<sub>34</sub>B<sub>8</sub>O<sub>6</sub> molecules corresponding to absorption maxima (λ<sub>max</sub>) at TDDFT, CNDO/S, and INDO/S levels.

Molecule	λ <sub>max</sub> /nm			E <sub>v</sub> /eV			f		
	TDDFT	CNDO/S	INDO/S	TDDFT	CNDO/S	INDO/S	TDDFT	CNDO/S	INDO/S
C <sub>22</sub> H <sub>32</sub> B <sub>10</sub> O <sub>6</sub>	204.69	246.29	207.62	6.06	5.02	5.97	0.11	0.74	0.12
C <sub>24</sub> H <sub>34</sub> B <sub>8</sub> O <sub>6</sub>	205.27	247.46	204.06	6.04	5.00	5.98	0.14	0.75	0.15

Table 3. Calculated highest occupied molecular orbital (H) and the lowest unoccupied molecular orbital (L) energies, energy gap  $E_g = E_L - E_H$ , ionisation energy  $I = (-E_H)$ , electron affinity  $A = (-E_L)$ , electro negativity  $\chi = (I + A)/2$ , chemical hardness  $\eta = (I - A)/2$ , electronic chemical potential  $\mu = -(I + A)/2$ , electrophilicity index  $\omega = \mu^2/\eta$ , and softness  $S = 1/\eta$  of the studied compounds using TDDFT, CNDO/S, and INDO/S levels.

Molecule	Method	H/eV	L/eV	$E_g$ /eV	I/eV	A/eV	$\chi$ /eV	$\eta$ /eV	$\mu$ /eV	$\omega$ /eV	$S$ /eV <sup>-1</sup>
C <sub>22</sub> H <sub>32</sub> B <sub>10</sub> O <sub>6</sub>	TDDFT	-8.75	-0.43	8.32	8.75	0.43	4.59	4.16	-4.59	5.06	0.24
	CNDO/S	-8.20	-2.59	5.61	8.20	2.59	5.39	2.80	-5.39	10.37	0.36
	INDO/S	-8.23	-0.60	7.63	8.23	0.60	4.41	3.81	-4.41	5.10	0.26
C <sub>24</sub> H <sub>34</sub> B <sub>8</sub> O <sub>6</sub>	TDDFT	-8.67	-0.61	8.06	8.67	0.61	4.64	4.03	-4.64	5.34	0.19
	CNDO/S	-8.56	-2.37	6.19	8.56	2.37	5.46	3.09	-5.46	9.65	0.32
	INDO/S	-8.15	-0.61	7.54	8.15	0.61	8.76	3.77	-4.38	5.09	0.20

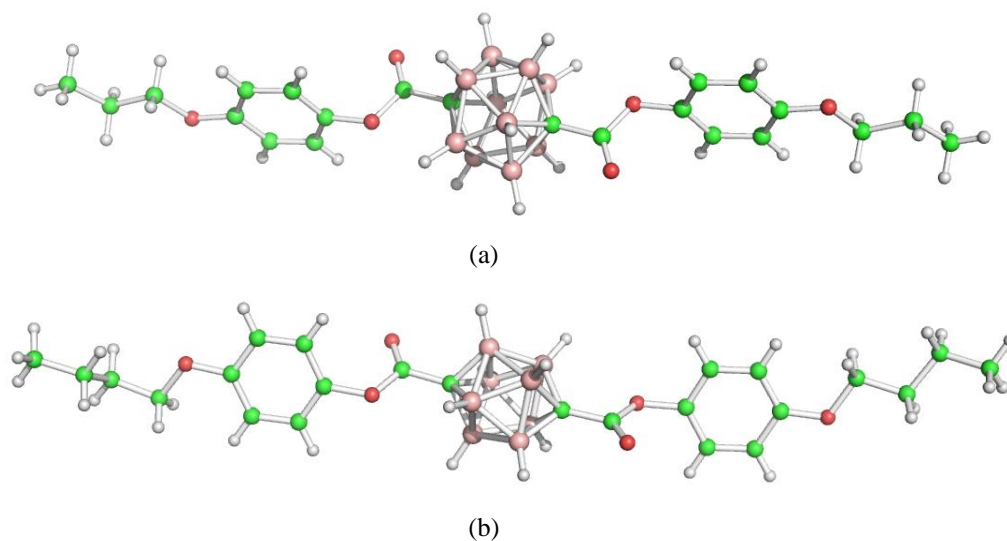


Fig. 1

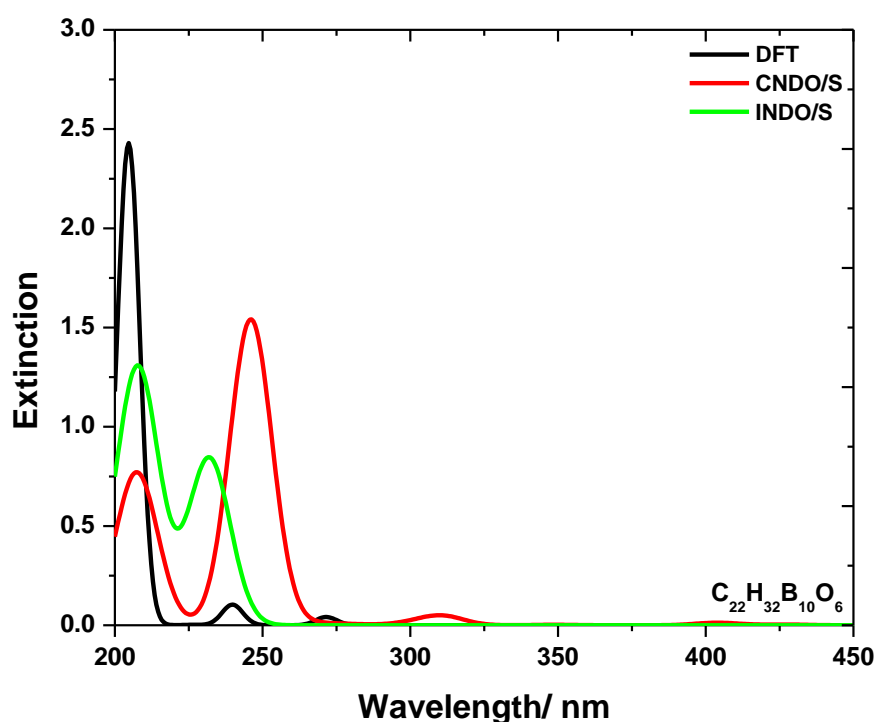


Fig. 2

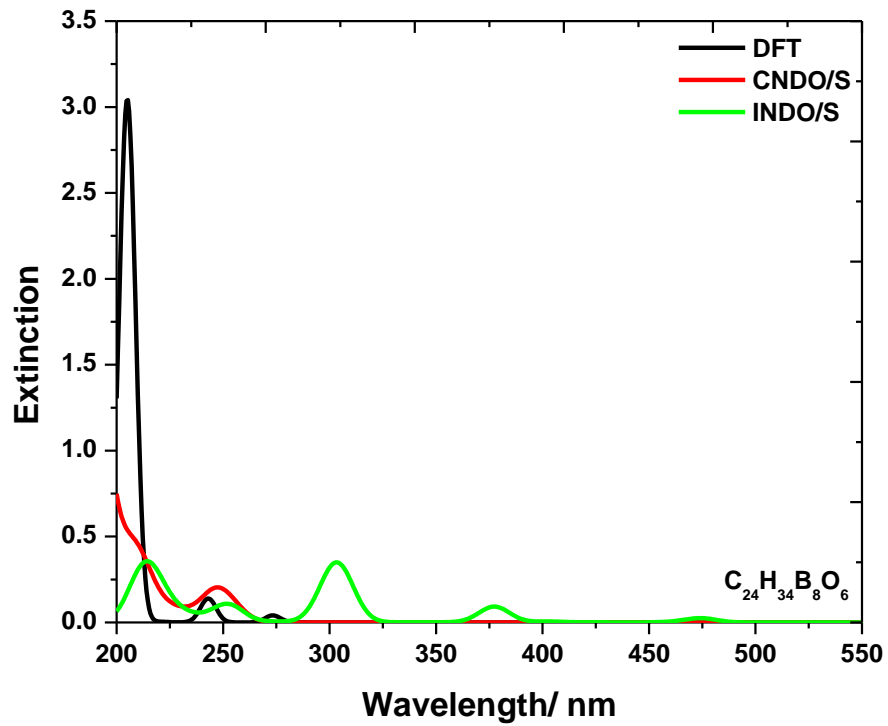


Fig. 3

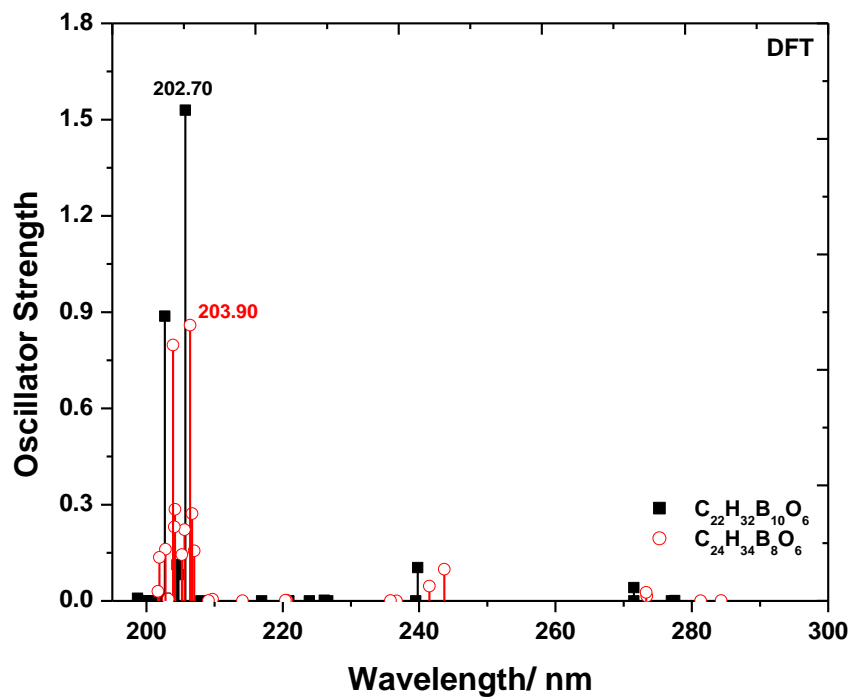


Fig. 4